Nanoscale

Cite this: *Nanoscale*, 2012, **4**, 1471

www.rsc.org/nanoscale

COMMUNICATION

Well-aligned ZnO nanowires with excellent field emission and photocatalytic properties†

Fu-Hsuan Chu,[a] Chun-Wei Huang,[a] Cheng-Lun Hsin,[a] Chun-Wen Wang,[a] Shih-Ying Yu,[a] Ping-Hung Yeh[b] and Wen-Wei Wu*[a]

Received 12th July 2011, Accepted 6th September 2011
DOI: 10.1039/c1nr10796h

Well-aligned ZnO nanowires (NWs) were successfully synthesized on Si(100) by the process of carbothermal reduction and vapor–liquid–solid method. Scanning electron microscopy and transmission electron microscopy results confirmed that ZnO NWs were single crystalline wurtzite structures and grew along the [0001] direction. The influences of substrate temperature and total pressure on the growth were discussed. The well-aligned ZnO NWs show good field emission properties, and the emitter constructed of pencil-like ZnO NWs exhibited a low turn-on field (3.82 V μm^{-1}) and a high field enhancement factor (β = 2303). Finally, we demonstrated that the as-prepared ZnO NWs with small diameter on the substrate have good photocatalytic activity toward degradation of methylene blue. Using ZnO NWs with Au nanoparticles (NPs) would decrease the recombination rate of hole–electron pairs due to the great shift of the Fermi level to the conduction band. Hence, adding Au NPs was a promising method to enhance the photocatalytic performance of ZnO NWs. It is significant that photocatalyst fabricated by ZnO NWs can apply to the degradation of organic pollution, and solve the environmental issues.

Introduction

ZnO nanostructures, such as nanobelts,[1,2] nanohelixes,[3] nanocombs,[4,5] nanosprings,[6] nanotubes,[7] nanowires,[8] and nanorings[9] have attracted increasing attention in recent years due to a wide band gap of 3.37 eV and a large bonding energy of 60 meV. The growth of ZnO nanostructures can be synthesized by various methods, such as vapor phase transport,[10] metal–organic chemical vapor deposition (MOCVD),[11] pulse-laser ablation,[12] a hydrothermal method,[13] and an electrochemical deposition technique.[14] Among the nanostructures, ZnO nanowires (NWs) have great potential applications in photoelectronic devices,[15,16] electronic devices,[17,18] dye-sensitized solar cells,[19] nanosensors,[20–22] and nanogenerators,[23] attributing to their high aspect ratio and chemical stability. The well-aligned ZnO NWs tend to improve the emission efficiency compared with randomly grown NWs. And the tipped structures of NWs could be beneficial for the application of field emission display, cathodoluminescence, antireflection and self-cleaning.[24–26] The surface effect also plays an important role in the device efficiency including solar cells and sensors.[27] Moreover, ZnO NWs could have potential applications as photocatalyst in environmental purification, for example, the organic contaminants can be decomposed by the photocatalytic reaction of ZnO NWs.

In this paper, we present the growth of well-aligned ZnO NWs using a carbothermal reduction method and a vapor–liquid–solid (VLS) mechanism on a Si substrate with a Au catalyst film. The shape of the ZnO NWs can be controlled by tuning growth parameters and the field-emission property can be enhanced. The pencil-like structure showed excellent field emission properties with a low turn-on field and a high field enhancement factor. Furthermore, Au-NP-functionalized ZnO NWs were synthesized. By controlling the diameter of Au NPs, the photodegradation will be enhanced due to the decrease in built-in potential and increase of the residual holes. With these results, we may provide some further information for ZnO nanostructure applications. The photocatalytic activity of ZnO NWs was studied by degradation of methylene blue (MB) with various diameters. For enhancement of the photocatalytic property, Au NPs were synthesized on the surface of ZnO NWs using a physical method. The effect of Au NP size on photodegradation of MB has been studied.

Experimental

The growth of well-aligned ZnO NWs was performed in a three-zone furnace using a carbothermal reduction method and VLS mechanism. The 3 nm-thick Au film was deposited on Si(100), which serves as a catalyst. The temperatures at different zones of the furnace were set at 950, 750 and 600 °C, respectively. ZnO and graphite powder were mixed with a weight ratio of 2 : 1 in an alumina boat at an upstream zone (950 °C) and the Si substrate was place at the midstream zone (750 °C). The flow rates of Ar and O_2 were adjusted to 100 sccm and 10 sccm, respectively. The chamber was pumped to the pressure of 0.75 Torr. The temperature was elevated at the rate of 10 °C min^{-1} and maintained at the highest temperature for 1.5 hour.

[a]*Department of Materials Science and Engineering, National Chiao Tung University, No. 1001, University Rd, East Dist, Hsinchu City, 300, Taiwan. E-mail: wwwu@mail.nctu.edu.tw; Fax: +886 3 5724727; Tel: +886 3 5712121 55395*
[b]*Department of Physics, Tamkang University, No. 151 Yingzhuan Rd, Danshui Dist, New Taipei City, 25137, Taiwan*
† This article was submitted as part of a collection highlighting papers on the 'Recent Advances in Semiconductor Nanowires Research' from ICMAT 2011.

The effect of the substrate temperature and chamber pressure on the morphology of ZnO NWs was investigated and the best condition for the growth of well-aligned ZnO NWs was expected and examined. The morphology and structure of ZnO NWs were characterized by JEOL 6500F scanning electron microscopy (SEM), X-ray diffraction (XRD) and JEOL 2100F high resolution transmission electron microscopy (HRTEM).

The field emission property of ZnO NWs with different morphologies was studied. The field emission measurement was carried out in a metallic ultrahigh vacuum system. The cathode and the anode were separated by spacers of 200 μm in thickness. Voltages up to 1.1 kV were applied between the anode and cathode and the *J–E* characteristics were measured to study the field emission properties.

The photocatalytic activity of ZnO NWs was characterized by degradation of methylene blue (MB). The ZnO NWs on the Si substrate were placed in a 10 ml of MB solution with 4×10^{-5} M under the UV light (UV Gremicidal Lamps, EYE, G10T8, 10 W) radiation. After irradiation for 30 min, the absorbance of MB was measured using a UV-vis spectrometer. The effect of photocatalytic activities on the structures, such as ZnO film, was compared with the as-grown samples with different diameters. For enhancement of the photocatalytic property, Au NPs were synthesized on the surface of ZnO NWs using a simple physical method. Au film was deposited on as-prepared ZnO NWs and annealed at 600 °C to aggregate to NPs on ZnO NWs. The efficiency of different Au NP sizes on the enhancement of photodegradation was also explored.

Results and discussion

Synthesis of ZnO NWs

ZnO NWs were grown vertically on the Si substrate with identical length as shown in Fig. 1(a). The length of well-aligned ZnO NWs is about 25 μm with a high aspect ratio ~250. The XRD pattern in Fig. 1(b) indicated that the peaks corresponded to (002), (101) and (102) planes of the wurtzite structure of ZnO. The intensity of the (002) plane was much stronger than the others, which was consistent with the SEM image showing ZnO NWs grown along one direction. The HRTEM image shown in Fig. 1(c) revealed that the ZnO NW was single crystalline with smooth surface. In compliance with the distance between atoms and the selective-area diffraction pattern, ZnO NWs exhibited the wurtzite structure and [0001] growth direction.

The ZnO nanostructures with different morphologies were grown at various substrate temperatures, as illustrated in Fig. 2. ZnO NWs with a high aspect ratio grew vertically on the substrate at 700 and 750 °C, as shown in Fig. 2(a) and (b), respectively. Since the Zn supersaturation point increases as the temperature increases, the precipitation cannot proceed with insufficient Zn vapor. The density of ZnO NWs decreased when the temperature was higher than 800 °C, as shown in Fig. 2(c). The ZnO nanoparticles or film would be formed at 850 °C, and the density of ZnO NWs was decreased as seen in Fig. 2(d).

The ZnO NW morphology would be variant due to the various pressures. The SEM images of ZnO NWs grown with different pressures of 0.75, 1, 2 and 3 Torr are shown in Fig. 3(a)–(d), respectively. With total pressure increasing, the partial pressure of Zn vapor was decreasing, the growth rate would be reduced and the length of ZnO NWs would also be decreased. On the other hand, the well-aligned ZnO NWs can be fabricated due to well controlling the partial pressure.

Field emission property

By tuning the growing parameters, the different shapes of ZnO NWs can be formed. The field emission property of two different tipped ZnO NWs vertically grown on Si substrates was measured. Planar-tipped ZnO NWs with uniform diameter of 180 nm (Fig. 4(a)) and pencil-like NWs with varied sizes 55, 85 and 170 nm in diameters from top to bottom were obtained. The pencil-like ZnO NWs show the great field emission property, the field emission current density–electrical field (*J–E*) curve is presented in Fig. 4(c). The turn-on fields, defined as the electrical field at the emission current density of 10 μA cm^{-2}, are 3.82 V μm^{-1} and 4.18 V μm^{-1} for pencil-like and planar-tipped structures, respectively. By controlling the ZnO NW shapes, the field-emission property can be enhanced. The field emission characteristics were theoretically evaluated by the Fowler–Nordheim (FN) equations

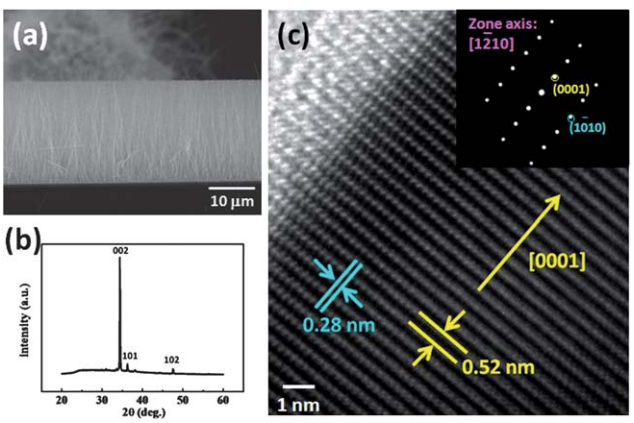

Fig. 1 (a) The SEM image of well-aligned ZnO NWs; (b) the XRD pattern of the as-grown sample; (c) the HRTEM image of ZnO NWs, exhibiting a single crystalline structure and the [0001] growth direction. The inset shows the corresponding diffraction pattern.

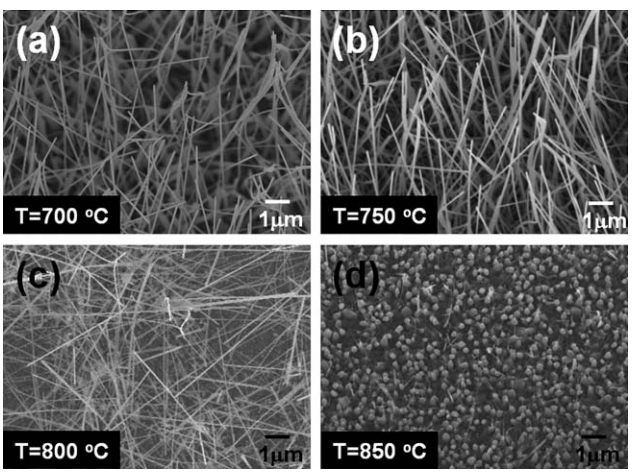

Fig. 2 SEM images of ZnO NWs grown under different temperatures: (a) 700 °C, (b) 750 °C, (c) 800 °C, and (d) 850 °C, respectively.

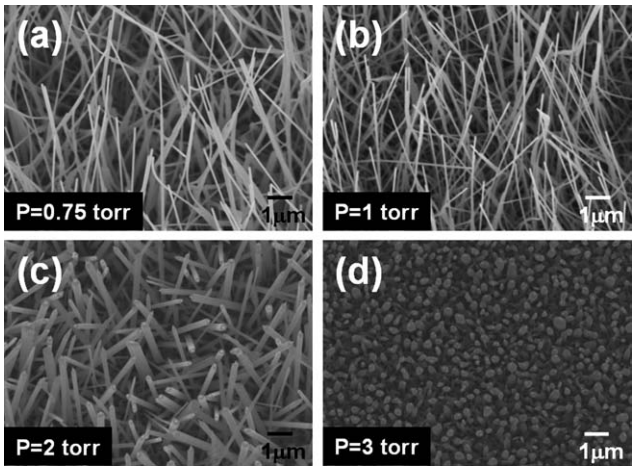

Fig. 3 SEM images of ZnO NWs grown under different chamber pressures: (a) 0.75 Torr, (b) 1 Torr, (c) 2 Torr, and (d) 3 Torr, respectively.

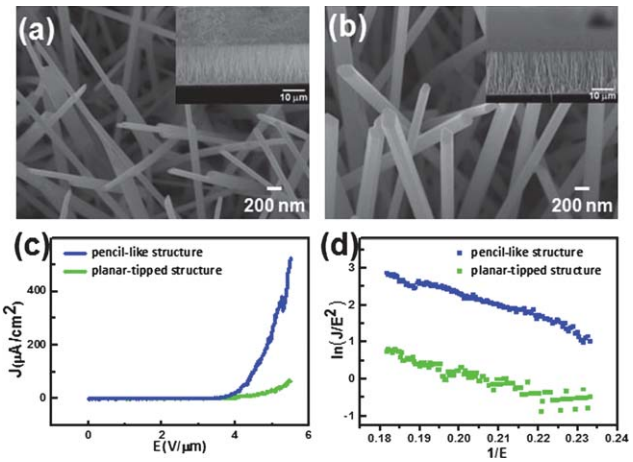

Fig. 4 SEM images of well-aligned ZnO NWs with different morphologies: (a) planar-tipped structure and (b) pencil-like structure. Field emission properties of ZnO NWs: (c) *J*–*E* curves and (d) corresponding Fowler–Nordheim plots of (c).

$$J(E) = AE^2\phi^{-1}\exp\left(\frac{-B\phi^{3/2}}{\beta E}\right) \quad (1)$$

or

$$\ln\frac{J}{E^2} = \ln A\phi^{-1} + \left(\frac{-B\phi^{3/2}}{\beta E}\right) \quad (2)$$

where A and B are constants with the value of 1.56×10^{-10} A V^{-2} eV and 6.83×10^3 V eV$^{-3/2}$ μm^{-1}, respectively. ψ is the work function of the emitter, which is 5.3 eV for ZnO. J is the current density in mA cm^{-2}, and E is the electrical field in V μm^{-1}. β is the field enhancement factor, which is related to the large aspect ratio of ZnO NWs. The field enhancement factor can be derived from the slope of $\ln(J/E^2)$–$(1/E)$ curve, called F–N plot in Fig. 4(d). The field enhancement factors of pencil-like and planar-tipped ZnO NWs are 2303 and 2095, respectively. The pencil-like structure of ZnO NWs has a higher field enhancement factor due to the advantage of the emitter geometry. Compared with the previous report of random ZnO NWs,[28] well-aligned structure has a higher field enhancement factor. Additionally, the pencil-like ZnO NWs also has lower turn-on field than the uniform ZnO NWs with small diameter.[29] The excellent emission characteristics were attributed to the aligned morphology and special geometry.

Photocatalytic activity

We also demonstrated that ZnO nanostructures can be used in the photocatalytic degradation application, in Fig. 5(a), the absorbance spectra of MB after the photocatalytic degradation by ZnO NWs with diameter of 60–80 nm under UV irradiation can be seen. The decrease in absorbance at a wavelength of 664 nm was observed with the increase of irradiation time. There would be no influence on absorbance without irradiation or ZnO NWs (not shown here). Hence, we can confirm the photocatalytic effect of ZnO NWs on the degradation of MB. The photocatalytic process was dominated by the following reactions:[30]

$$\mathrm{ZnO} + h\nu \rightarrow \mathrm{ZnO}(e^-_{cb} + h^+_{vb}) \quad (3)$$

$$h^+_{vb} + \mathrm{OH}^- \rightarrow {}^{\cdot}\mathrm{OH} \quad (4)$$

$$h^+_{vb} + \mathrm{H_2O} \rightarrow {}^{\cdot}\mathrm{OH} + \mathrm{H}^+ \quad (5)$$

$${}^{\cdot}\mathrm{OH} + \mathrm{MB} \rightarrow \text{degradation of MB} \quad (6)$$

under UV irradiation, ZnO NWs obtained energy and induced electron–hole pairs through the photogeneration process (eqn (3)). The strong oxidative hydroxyl radicals (˙OH) were formed by the

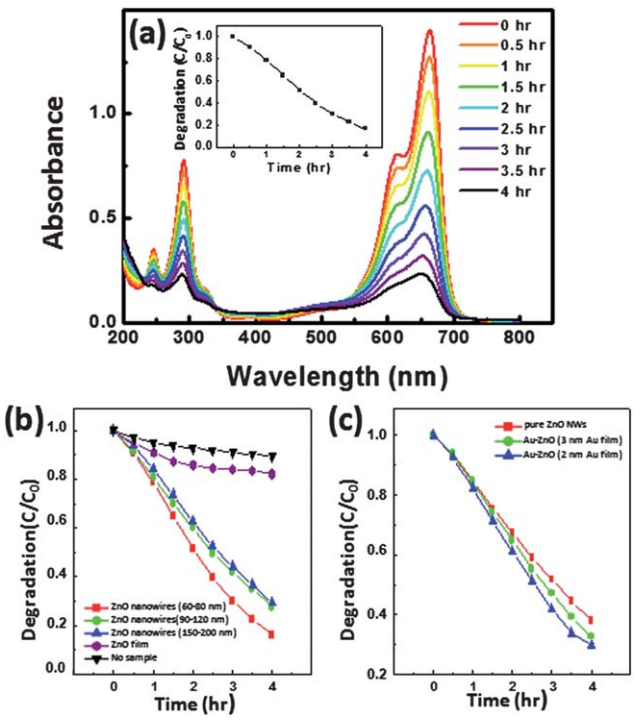

Fig. 5 (a) Absorbance spectra of MB as a function of irradiation time after the photocatalytic degradation by ZnO NWs. The inset shows photodegradation of MB. (b) Photodegradation of MB using various ZnO nanostructures. (c) Photodegradation of MB using ZnO NWs with various sizes of Au NPs.

reaction between holes and hydroxyl group (OH^-) at the ZnO surface (eqn (4)). H_2O could also react with holes to form hydroxyl radicals (eqn (5)). The hydroxyl radical was regarded as a strong oxidant, leading to the oxidation of dye, and the degradation of MB was observed.

The effect of photocatalytic properties with different morphologies was investigated. ZnO NWs have great photocatalytic properties in comparison with the ZnO film due to the large surface area as shown in Fig. 5(b). Moreover, ZnO NWs with smaller diameter (60–80 nm) exhibited better performance of the photocatalytic degradation than NWs of larger diameter (150–200 nm). It was indicated that surface area could play a significant role on the efficiency of photocatalysis since photocatalytic reaction occurred on the surface.

The limit of photocatalytic activity is the high recombination rate of photogenerated electron–hole pairs. In order to decrease the recombination rate, it was suggested to form heterojunction between the noble metal and semiconductor. In our study, we selected Au NPs and used an effective method to form heterojunctions. Au thin film was deposited on the substrate with ZnO NWs (60–80 nm in diameter) using electron gun deposition and then annealed at 600 °C. Au NPs with the diameter of 3 nm were formed on the surface of ZnO NWs by depositing 2 nm Au film, as shown in Fig. 6(a). With the deposition of a 3 nm Au film, the NPs with the diameter of 8 nm were formed, as shown in Fig. 6(b). Fig. 6(c) and (d) show the EDS results which indicate the presence of Au elements in Fig. 6(a) and (b). The photocatalytic activity of ZnO NWs with 60–80 nm in diameter with different size of Au NPs in comparison with pure ZnO NWs is shown in Fig. 5(c). It is remarkable that the Au NPs effectively enhance the photodegradation rate of MB. In addition, the NPs with smaller size have better enhancement of photocatalytic activity. It was suggested that the behavior of Au NPs is similar to the quantum dot, when in contact with ZnO and the depletion layer was formed on the ZnO surface due to the Schottky barrier between ZnO NWs and Au NPs. The controlled size of Au NPs was found to effectively enhance the photodegradation rate of MB, and dominate the photocatalytic properties more than the density of Au NPs. In addition, a larger shift of the Fermi level was formed with the smaller size of Au NPs, resulting in the decrease of the built-in potential.[31,32] Thus electrons can be reserved in Au NPs and the recombination rate of electron–hole pairs would be decreased, finally the photodegradation rate was enhanced with the increase of the residual holes.

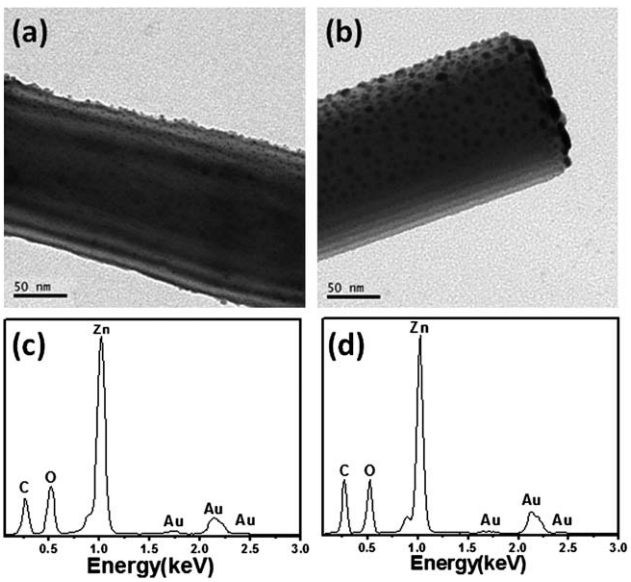

Fig. 6 Low-magnification TEM images of Au NPs synthesized by depositing different thicknesses of Au film: (a) 2 nm Au film and (b) 3 nm Au film, respectively. (c) and (d) Corresponding EDS analysis of (a) and (b), respectively.

Conclusions

Well-aligned ZnO NWs were synthesized successfully on a Si substrate using a carbothermal reduction and VLS mechanism. The effects of substrate temperature and chamber pressure on the growth of ZnO nanostructures were investigated. The ZnO NWs with high aspect ratio and density were observed at specific temperature (750 °C) and pressure (0.75 Torr). The ZnO NWs exhibited a single crystalline wurtzite structure with the [0001] growth direction. The well-aligned ZnO NWs displayed good field emission properties in comparison with random ZnO NWs. Moreover, the pencil-like ZnO NWs showed low turn-on field (3.82 V μm^{-1}) and high field enhancement factor ($\beta = 2303$). The photodegradation of MB under UV irradiation was performed to investigate the photocatalytic activity of ZnO. Compared with the ZnO film, the as-prepared ZnO NWs have good photocatalytic activity, and the smaller diameter ZnO NWs show better photocatalytic property. Furthermore, the enhancement of the photodegradation was observed with the Au NPs formed on the surface of ZnO NWs. The smaller size of Au NPs induced a larger shift of the Fermi level, leading to the decrease in recombination rate of the photogenerated electron–hole pairs. By controlling the diameter of Au NPs, the photodegradation will be enhanced due to the decrease in built-in potential and increase of the residual holes.

Acknowledgements

The authors would like to acknowledge the support by the ROC National Science Council through grant no. NSC 97-2218-E-009-027-MY3 and NSC 98-2112-M-032-003-MY3.

Notes and references

1 Z. W. Pan, Z. R. Dai and Z. L. Wang, *Science*, 2001, **291**, 1947–1949.
2 Z. L. Wang, *Mater. Sci. Eng., R*, 2009, **64**, 33–71.
3 P. X. Gao, Y. Ding and Z. L. Wang, *Nano Lett.*, 2009, **9**, 137–143.
4 Z. L. Wang, X. Y. Kong and J. M. Zuo, *Phys. Rev. Lett.*, 2003, **91**, 185502.
5 Y. H. Zhang, X. B. Song, J. Zheng, H. H. Liu, X. G. Li and L. P. You, *Nanotechnology*, 2006, **17**, 1916–1921.
6 X. Y. Kong and Z. L. Wang, *Appl. Phys. Lett.*, 2004, **84**, 975–977.
7 H. D. Yu, Z. P. Zhang, M. Y. Han, X. T. Hao and F. R. Zhu, *J. Am. Chem. Soc.*, 2005, **127**, 2378–2379.
8 Y. W. Heo, D. P. Norton, L. C. Tien, Y. Kwon, B. S. Kang, F. Ren, S. J. Pearton and J. R. LaRoche, *Mater. Sci. Eng., R*, 2004, **47**, 1–47.
9 Z. L. Wang, X. Y. Kong, Y. Ding, P. X. Gao, W. L. Hughes, R. S. Yang and Y. Zhang, *Adv. Funct. Mater.*, 2004, **14**, 943–956.
10 M. H. Huang, Y. Y. Wu, H. Feick, N. Tran, E. Weber and P. D. Yang, *Adv. Mater.*, 2001, **13**, 113–116.
11 W. Lee, M. C. Jeong and J. M. Myoung, *Acta Mater.*, 2004, **52**, 3949–3957.
12 Y. Sun, G. M. Fuge and M. N. R. Ashfold, *Superlattices Microstruct.*, 2006, **39**, 33–40.
13 Y. Tak and K. J. Yong, *J. Phys. Chem. B*, 2005, **109**, 19263–19269.
14 M. J. Zheng, L. D. Zhang, G. H. Li and W. Z. Shen, *Chem. Phys. Lett.*, 2002, **363**, 123–128.

15 M. T. Chen, M. P. Lu, Y. J. Wu, J. H. Song, C. Y. Lee, M. Y. Lu, Y. C. Chang, L. J. Chou, Z. L. Wang and L. J. Chen, *Nano Lett.*, 2010, **10**, 4387–4393.
16 J. H. He, S. T. Ho, T. B. Wu, L. J. Chen and Z. L. Wang, *Chem. Phys. Lett.*, 2007, **435**, 119–122.
17 P. C. Chang and J. G. Lu, *IEEE Trans. Electron Devices*, 2008, **55**, 2977–2987.
18 J. H. He, P. H. Chang, C. Y. Chen and K. T. Tsai, *Nanotechnology*, 2009, **20**, 135701.
19 M. Law, L. E. Greene, J. C. Johnson, R. Saykally and P. D. Yang, *Nat. Mater.*, 2005, **4**, 455–459.
20 T. Y. Wei, P. H. Yeh, S. Y. Lu and Z. L. Wang, *J. Am. Chem. Soc.*, 2009, **131**, 17690–17695.
21 P. H. Yeh, Z. Li and Z. L. Wang, *Adv. Mater.*, 2009, **21**, 4975–4978.
22 D. Zhu, Q. He, Q. Chen, Y. Fu, C. He, L. Shi, X. Meng, C. M. Deng, H. M. Cao and J. G. Cheng, *ACS Nano*, 2011, **5**(6), 4293–4299.
23 Z. L. Wang, *Adv. Funct. Mater.*, 2008, **18**, 3553–3567.
24 L. K. Yeh, K. Y. Lai, G. J. Lin, P. H. Fu, H. C. Chang, C. A. Lin and J. H. He, *Adv. Energy Mater.*, 2011, **1**, 506–510.
25 J. H. He, R. S. Yang, Y. L. Chueh, L. J. Chou, L. J. Chen and Z. L. Wang, *Adv. Mater.*, 2006, **18**, 650–654.
26 Y. R. Lin, K. Y. Lai, H. P. Wang and J. H. He, *Nanoscale*, 2010, **2**, 2765–2768.
27 C. Y. Chen, M. W. Chen, J. J. Ke, C. A. Lin, J. R. D. Retamal and J. H. He, *Pure Appl. Chem.*, 2010, **82**, 2055–2073.
28 Y. Q. Chang, X. H. Chen, H. Z. Zhang, W. J. Qiang and Y. Long, *J. Vac. Sci. Technol., B: Microelectron. Nanometer Struct.–Process., Meas., Phenom.*, 2007, **25**, 1249–1252.
29 Y. Zhang and C. T. Lee, *J. Phys. Chem. C*, 2009, **113**, 5920–5923.
30 H. C. Yatmaz, A. Akyol and M. Bayramoglu, *Ind. Eng. Chem. Res.*, 2004, **43**, 6035–6039.
31 J. J. Wu and C. H. Tseng, *Appl. Catal., B*, 2006, **66**, 51–57.
32 V. Subramanian, E. E. Wolf and P. V. Kamat, *J. Phys. Chem. B*, 2003, **107**, 7479–7485.